

Electronic structure and magnetism of RMn_6Sn_6 ($R = Tb, Dy$)^{*}

TAN Ming-qiu(谭明秋), TAO Xiang-ming(陶向明), HE Jun-hui(何军辉), CAO Song(曹松)

(Department of Physics, Zhejiang University, Hangzhou 310027, China)

Received Nov. 25, 2000; Revision accepted July 6, 2001

Abstract: This article reports first-principles band structure calculations for RMn_6Sn_6 ($R = Tb, Dy$). The calculation uses the linear muffin-tin orbitals (LMTO) method in the atomic-sphere-approximation (ASA), and yields results showing that both $TbMn_6Sn_6$ and $DyMn_6Sn_6$ are ferrimagnetic compounds with antiparallel aligned moments of R and Mn atoms. In this research the $4f$ states of R atoms are treated as localized states, i.e., the hybridization of $4f$ states with other valence electrons is neglected. The moments of Mn in both compounds were determined to be $2.43 \mu_B$ and $2.38 \mu_B$, respectively. The considerably small additional moments for Mn from the spin-orbit coupling indicates that the spin-orbital coupling is not dominated for Mn atoms. The total moments of Tb and Dy atoms are $10.28 \mu_B$ and $11.20 \mu_B$. All the calculation findings accorded well with experimental results.

Key words: rare earth, *ab initio* band structure, atomic sphere approximation

Document code: A

CLC number: O481.1; O482.5

INTRODUCTION

Malaman et al. (1988) reported the crystallographic data and magnetic properties of new ternary stannides RMn_6Sn_6 ($R = Sc, Y, Gd-Tm, Lu$). Chafik El Idrissi et al., 1991a; Chafik El Idrissi et al., 1991b; Venturini et al., 1993a; Venturini et al., 1993b; Venturini et al., 1996) All these compounds crystallize in the $HfFe_6Ge_6$ -type structure (No. 191, $P6/mmm$) that can be described as built of alternate (001) layers containing R and transition metal atoms, respectively. R elements build hexagonal planes and transition metal atoms Kagomê nets stacked along the c -axis. As regards the transition metal and rare earth this structure is also closely related to the well-known $CaCu_5$ and $ThMn_{11}$ -type structures. Fig.1 shows the crystalline structure in this study.

Magnetic measurements (Venturini et al., 1991) showed that $GdMn_6Sn_6$, $TbMn_6Sn_6$, $DyMn_6Sn_6$ and $HoMn_6Sn_6$ display ferrimagnetic behavior below $T_C = 435, 423, 393$ and 376 K, respectively. Furthermore, except for $GdMn_6Sn_6$,

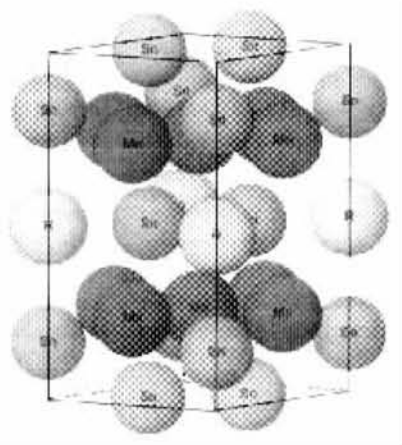


Fig.1 Crystalline structure of RMn_6Sn_6
($R = Tb, Dy$)

these compounds exhibit an additional transition (at $T_t = 330, 240$ and 180 K, for Tb, Dy, and Ho, respectively) which could be related to a change in their easy axis direction. In contrast, $ErMn_6Sn_6$, behaves antiferromagnetically below $T_N = 352$ K and a second-order magnetic transition to a ferrimagnetic state occurs at 75 K.

Neutron diffraction experiments on some of these compounds (Chafik El Idrissi et al., 1991) demonstrated clearly that the ferrimagnetism is caused by an anti-ferromagnetic arrangement of rare earth (R) and Mn moments. In a recent research Malaman et al. (1999) presented the neutron diffraction on magnetic structures of $GdMn_6Sn_6$ (at 2 K and 280 K), $TbMn_6Sn_6$ (above room temperature, i.e., between T_i and T_c), $DyMn_6Sn_6$ (between 2 K and T_c) and $ErMn_6Sn_6$ (below 75 K).

In this work, we performed a first-principles band structure calculation on $TbMn_6Sn_6$ and $DyMn_6Sn_6$ to determine the band features near Fermi energy, and the magnetism and moments in these compounds, because in most cases the physical properties of solids are dominated by the electronic states near Fermi energy. At the same time, we intended to check the validity of our calculation efforts on special treatment of nearly localized 4f states in rare earth compounds.

CALCULATION DETAILS

In this work, we used a relativistic version of LMTO-ASA scheme (Andersen et al., 1976). The spin-orbital coupling (SOC) for heavy elements such as Tb and Dy was treated as a first order perturbation. We used the experimental crystalline data near 0 K in this work. $Tb(6s, 6p, 5d)$, $Dy(6s, 6p, 5d)$, $Mn(4s, 4p, 3d)$, and $Sn(5s, 5p)$ were treated as valence states where frozen-core approximation was applied to the deeply bound core levels. During self-consistent calculation, the one-center expansion of charge density and potential were expanded up to $l_{max} = 4$. The Fermi level was determined by the usual linear tetrahedron integration technique (Jepsen et al., 1971) in Brillouin zone (BZ). Furthermore, as for the exchange-correlation energy and potential, we took the form proposed by von Barth and Hedin (von Barth et al., 1972). In order to reach necessary numerical precision, we used 1326 k -points within the irreducible wedge of BZ (1/24 of hexagonal BZ). The numerical accuracy for charge density and total energy are 10^{-6} e/a.u.³ and 10^{-6} Ryd, respectively. The convergence of energy band eigenvalues and related parameters

was ensured by increasing the k -points in irreducible BZ.

RESULTS AND DISCUSSION

Figs. 2 and 3 are the plotted band structures and density of states plots for $TbMn_6Sn_6$ and $DyMn_6Sn_6$, respectively. Before we discuss our own results, we would like to mention the problem concerning the special treatment on 4f states of rare earth elements such as terbium and dysprosium. It is well known that the interaction between 4f states of individual R atoms are well screened by conduction bands due to the small effective radius of 4f electrons. In the so-called late rare earth (Gd-Yb) cases the 4f states form a narrow band without interaction with other valence electrons even though their energy levels are quite close to each other. In order to account for this observation, one usually regards the 4f states as partially occupied core states from the viewpoint of the "open core" technique as used in our previous research (Bin et al., 1986). For some ideal cases corresponding to Hund's rules, e.g., empty, half filled and fully filled 4f shell, we just needed to fix the number of 4f electrons as 0, 7 or 14 in practice. However, for the rare earth atoms with 4f shell deviating from the ideal Hund's rules (Hund, 1927) case, it is difficult to determine the number of 4f electrons constrained as core states. Usually, this difficulty could be overcome by fixing this number to the number of 4f electrons in an individual R atom. As free atoms, the valence electron configuration of Tb and Dy are $4f^8 5d^1 6s^2$ and $4f^{10} 5d^0 6s^2$, respectively. In accordance with the above analysis, it seems that one should take the 4f electrons as 8 and 10 for Tb and Dy in calculation. This treatment caused an unphysical consequence on the position of the occupied 4f levels for $DyMn_6Sn_6$. If we decreased the number of constrained 4f states to 9, the computed results were satisfactory as expected. This finding indicates that one of the 4f electrons in Dy is between well-localized f states and fully itinerant valence electrons in character.

In relation to the calculation of moments, one has to sum up the components from the valence electrons and partially occupied core states. Usually the orbital part of moment from

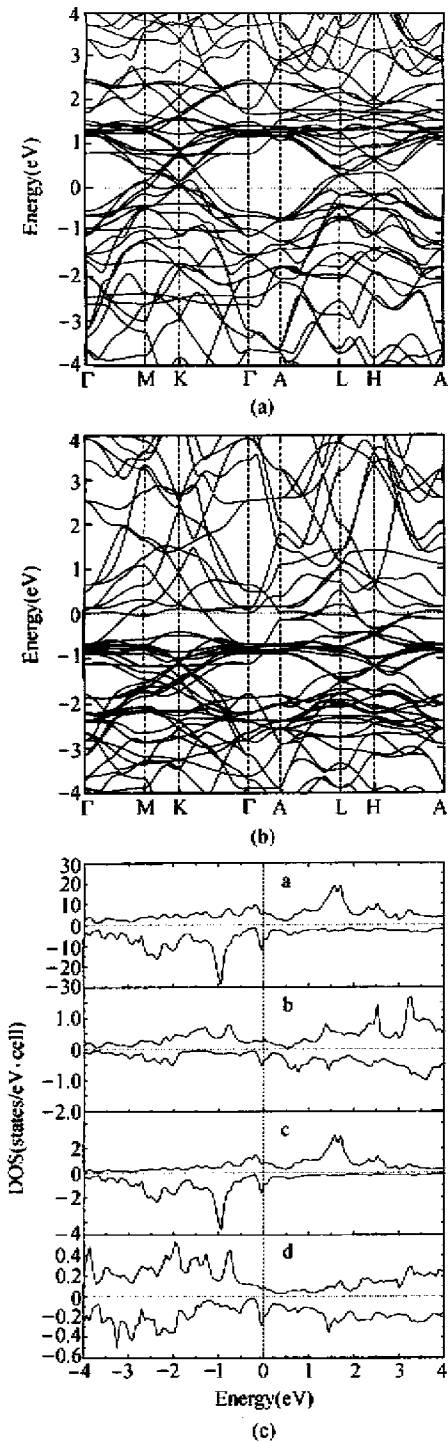


Fig.2 LSDA band-structures and DOS for TbMn_6Sn_6 (The energy zero is set to Fermi energy).

(a) spin-up bands; (b) spin-down bands; (c) DOS
(panel a: total DOS; panel b: partial DOS of Tb;
panel c: partial DOS of Mn; panel d: partial DOS of Sn)

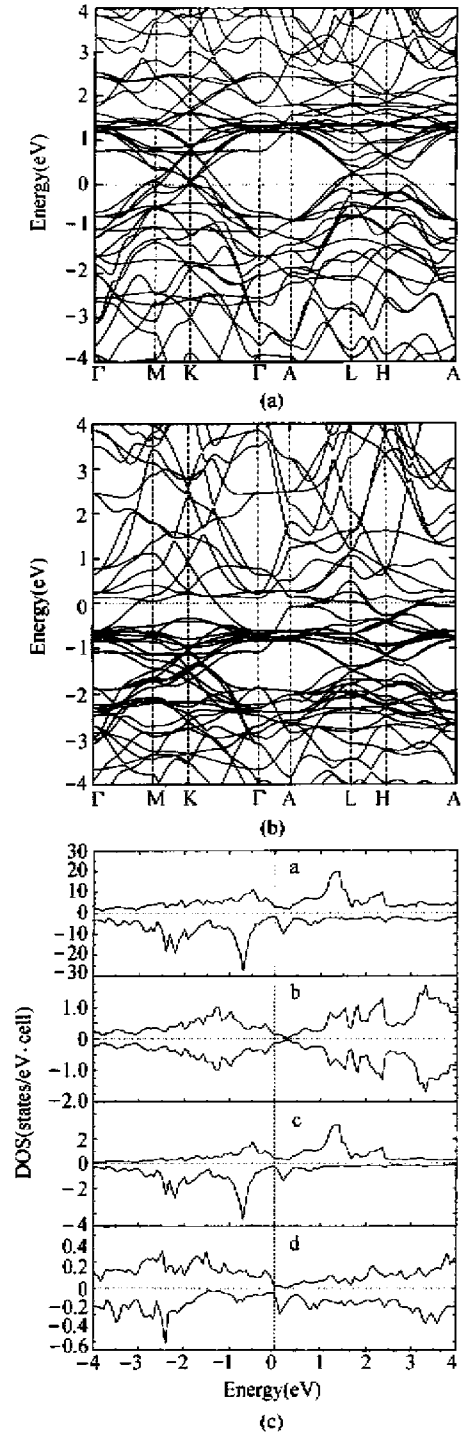


Fig.3 LSDA band-structures and DOS for DyMn_6Sn_6 (The energy zero is set to Fermi energy).

(a) spin-up bands; (b) spin-down bands; (c) DOS
(panel a: total DOS; panel b: partial DOS of Dy;
panel c: partial DOS of Mn; panel d: partial DOS of Sn)

valence states is small even if the spin-orbital coupling is included. From the calculated results on $TbMn_6Sn_6$ and $DyMn_6Sn_6$, we found that the orbital part of moment from valence states was moderately small. For the moment from partially occupied $4f$ states, we employed the formalism of L-S coupling and Hund's rules. Actually it reads

$$\mu_J = g_J \sqrt{J(J+1)} \mu_B,$$

where J is the total angular moment of partially occupied $4f$ states and g_J is called Landé factor. According to atomic physics (Hakken et al., 1984), Landé factor is written as

$$g_J = 1 + \frac{J(J+1) + S(S+1) - L(L+1)}{2J(J+1)},$$

where L is the orbital part of angular moment of incompletely filled $4f$ electrons in connection with Hund's rules.

According to our calculation results, the ground states of $TbMn_6Sn_6$ and $DyMn_6Sn_6$ are those of the ferrimagnetic structures, i. e., the moments of R and Mn atoms are anti-parallelly aligned. The spin moments were computed to be $6.56 \mu_B$ and $5.56 \mu_B$ for Tb and Dy, respectively. If the L-S coupling of partially occupied $4f$ states was included, the total moments would be $10.28 \mu_B/Tb$ and $11.20 \mu_B/Dy$. It is noted that the latter is quite close to the experimental value at 2 K for Dy (Malaman et al., 1999). However, for $TbMn_6Sn_6$, only the experimental moment for Tb near 305 K was available for comparison, so it was difficult to compare our result with experimental result directly because the calculation of band structure is correlated with the electronic structure of ground state only. In considering the variation tendency of Dy moment in $DyMn_6Sn_6$ (Malaman et al., 1999), it is reasonable to speculate that our prediction on the moment of Tb in $TbMn_6Sn_6$ is acceptable. The moments of the Mn atoms were determined to be $2.43 \mu_B$ and $2.38 \mu_B$, respectively. This observation is quite similar to that of MnAs, MnSb, and MnBi (Tan et al., 2000), in which the moment of Mn varies from $3.16 \mu_B$ to $3.66 \mu_B$. We suppose this minor difference is caused by the change of exchange and correlation potential in the L(S)DA calculation. We found the orbital part of the Mn moment is very small in both ma-

terials.

The band structures near Fermi level were dominated by the hybridization between Mn 3d bands and Sn 5p bands. Of course, the $5d$ bands of R atoms play a minor role in the band formation in this region. This conclusion can be drawn also from the density of states (see Fig. 2 (c) and 3(c)) easily. The peaks above Fermi level in the spin-down bands had Mn 3d character. It is interesting to note that this feature was common for both compounds.

The next important issue to be addressed here is the amplitude of hybridization of the $4f$ states with the $5d$ states of rare earth atoms. Due to the adequately small extent of $4f$ states, it is reasonable to neglect the hybridization between $4f$ states and the rest of the valence electrons of adjunct atoms such as Mn and Sn in this study. However, the intra-atom interaction between $4f$ states and $5d$ states, as expected, will lead to the valence band formation even though this hybridization is extremely small in most cases. In order to estimate the magnitude of the hybridization, we would like to mention the numeric test by Pethkhov et al. (Pethkhov et al., 1996) in dealing with the compounds $R-V$ ($R = Gd, Er$; $V = N, P, As$). The model Hamiltonian expression including the hybridization reads

$$\begin{aligned} \hat{H} = & \sum_{i\sigma} \epsilon_d d_{i\sigma}^+ d_{i\sigma} + \sum_{i\sigma} \epsilon_f f_{i\sigma}^+ f_{i\sigma} + \\ & V_{df} \sum_{\langle ij \rangle} \sum_{\sigma} (d_{i\sigma}^+ f_{j\sigma} + f_{j\sigma}^+ d_{i\sigma}) + \\ & V_{dd} \sum_{\langle ij \rangle} \sum_{\sigma} (d_{i\sigma}^+ d_{j\sigma} + d_{j\sigma}^+ d_{i\sigma}) + \\ & \frac{U}{2} \sum_{i\sigma} (\hat{n}_{j\sigma} \hat{n}_{j\bar{\sigma}} - n_j \hat{n}_{j\sigma}). \end{aligned}$$

The f level broadens into a band given by

$$E_f = \epsilon_f + \frac{[2V_{df} \sum_{\sigma} \cos(k_a a)]^2}{\epsilon_d + 2V_{dd} \sum_{\sigma} \cos(k_a a) - \epsilon_f},$$

with width

$$W_f = \frac{NV_{df}^2}{\epsilon_d \pm NV_{dd} - \epsilon_f},$$

where the $+$ ($-$) prevails if $V_{dd} > 0$ (< 0). Obviously, the $4f'$'s effect on the valence band is not essential if the energy difference between ϵ_d and ϵ_f is sufficient. This observation implies that one can omit the $4f'$'s when focusing on the fundamental features of electronic band structure in the compounds and alloys containing later $4f$

rare earth atoms. The review article by Campagna et al. (Campagna et al., 1979) dealt with the XPS spectra of various $4f$ elements. From those XPS spectra, one could immediately recognize the sharp localized characters of $4f$ states in spectra of later rare earth atoms.

CONCLUSIONS

In summary, we calculated the band structures of ferrimagnetic TbMn_6Sn_6 and DyMn_6Sn_6 by the *ab initio* LMTO-ASA method. To our knowledge, this is the first calculation try on the electronic structure and magnetism for these compounds. In this study we applied "open core" treatment on nearly localized $4f$ states and obtained satisfactory results on magnetic moments and electronic structure for both materials. Our results showed that the localized picture of $4f$ states is a good starting point for the proper description of late rare earth compounds in principle, at least in the case of the compounds discussed above.

References

- Andersen, O. K., 1975. Linear methods in band theory. *Phys. Rev.*, **B12**: 3060 – 3083.
- Bin, M. I., Jansen, H. J. F., Oguchi, T., et al., 1986. Total-energy local-density studies of the α - γ phase transition in Ce. *Phys. Rev.*, **B34**: 369 – 378.
- Campagna, M., Werrheim, C. K., Bear, Y., 1979. Photoemission in Solids, Vol. II, edited by Ley L. and Cardona M. Berlin, Springer-Verlag.
- Chafik El Idrissi, B., Venturini, C., Malaman, B., 1991a. Refinement of HfFe_6Ce_6 isostructural ScMn_6Sn_6 and TbMn_6Sn_6 . *Mater. Res. Bull.*, **26**: 431 – 437.
- Chafik El Idrissi, B., Venturini, C., Malaman, B., et al., 1991b. Magnetic structures of TbMn_6Sn_6 and HoMn_6Sn_6 compounds from neutron diffraction study. *Less-Common Met.*, **175**: 143 – 154.
- Hakken, H., Wolf, H. C., 1984. Atomic and Quantum Physics. Berlin Springer-Verlag.
- Hund, F., 1927. Linienspektren und periodisches der Elements. Berlin: Julius Springer.
- Jepsen, O., Andersen, O. K., 1971. The electronic structure of h. c. p. Ytterbium. *Solid State Commun.*, **9**: 1763 – 1767.
- Malaman, B., Venturini, C., Roques, B., 1988. New ternary stannides: MMn_6Sn_6 ($M = \text{Sc}, \text{Y}, \text{Sm}, \text{Cd-Tm}, \text{Lu}$) and ScFe_6Sn_6 . *Mater. Res. Bull.*, **23**: 1629 – 1633.
- Malaman, B., Venturini, G., Welter, R., et al., 1999. Magnetic properties of RMn_6Sn_6 ($R = \text{Cd-Er}$) compounds from neutron diffraction and Mössbauer measurements. *J. Magn. Magn. Mater.*, **202**: 519 – 534.
- Pethkhor, A. G., Lambrecht, W. R. L., Segall, B., 1996. Electronic structure of rare earth pnictides. *Phys. Rev.*, **B53**: 4324 – 4339.
- Tan, M. Q., Tao, X. M., Bao, S. N., 2000. *Ab initio* study on the electronic structure and magnetism of MnAs , MnSb , and MnBi . *Chin. Phys.*, **9**: 55 – 60.
- Venturini, G., Welter, R., Malaman, B., 1993a. Room temperature variation in the threshold fields in $\text{R}_x\text{Y}_{1-x}\text{Mn}_6\text{Sn}_6$ ($R = \text{Ce-Nd}, \text{Sm}, \text{Cd-Ho}$) solid solutions. *J. Alloys & Compounds*, **197**: 101 – 104.
- Venturini, G., Welter, R., Ressouche, E., et al., 1993b. Magnetic structure of YMn_6Ce_6 and room temperature magnetic structure of LuMn_6Sn_6 obtained from neutron diffraction study. *J. Alloys & Compounds*, **200**: 51 – 57.
- Venturini, G., Fruchart, D., Malaman, B., 1996. Incommensurate magnetic structures of RMn_6Sn_6 ($R = \text{Sc}, \text{Y}, \text{Lu}$) compounds from neutron diffraction study. *J. Alloys & Compounds*, **236**: 102 – 110.
- Von Barth, U., Hedin, L., 1972. A local exchange-correlation potential for the spin polarized Case: I. *J. Phys.*, **C5**: 1629 – 1642.